

TGF β -activated kinase-1 knockdown in hematopoietic stem-progenitor cells causes PANoptosis and myelodysplastic syndrome-like disease in mice

Lei Zhang,¹⁻³ Wenyan Li,⁴ Rohit Thalla,^{2,3} Rongyao Ma,¹ Ryan Mack,^{2,3} Ameet R. Kini,⁵ Austin Runde,^{2,3} Patrick A. Hagen,^{2,6} Kevin Barton,^{2,6} Jorgena Kost-Schwartz,^{2,5} Peter Breslin,^{2,3,7} Hong-Long Ji⁸ and Jiwang Zhang^{2,3,5}

¹Cyrus Tang Hematology Center, Collaborative Innovation Center of Hematology, National Clinical Research Center for Hematologic Diseases, MOE Engineering Center of Hematological Disease, Soochow University, Suzhou, China; ²Oncology Institute, Cardinal Bernardin Cancer Center, Loyola University Chicago Medical Center, Maywood, IL, USA; ³Department of Cancer Biology, Loyola University Chicago Medical Center, Maywood, IL, USA; ⁴Lanzhou University Second Hospital, Key Laboratory of Urological Diseases in Gansu Province, Lanzhou, Gansu, China; ⁵Departments of Pathology and Radiation Oncology, Loyola University Chicago Medical Center, Maywood, IL, USA; ⁶Department of Medicine, Loyola University Chicago Medical Center, Maywood, IL, USA; ⁷Departments of Biology and Molecular/Cellular Physiology, Loyola University Chicago, Maywood, IL, USA and ⁸Department of Surgery, Loyola University Chicago Medical Center, Maywood, IL, USA

Correspondence: J. Zhang
jzhang@luc.edu

Received: April 7, 2025.

Accepted: October 20, 2025.

Early view: October 30, 2025.

<https://doi.org/10.3324/haematol.2025.287951>

©2026 Ferrata Storti Foundation

Published under a CC BY-NC license



Abstract

Mutant *SF3B1* (*SF3B1^{mut}*) in hematopoietic stem/progenitor cells (HSPC) primarily affects erythropoiesis, resulting in myelodysplastic syndromes (MDS) with refractory macrocytic anemia and ring sideroblasts. *SF3B1^{mut}* results in aberrant splicing of a large number of transcripts in HSPC due to the alternative use of cryptic splice sites. Aberrant splicing of *Tmem14c* and *Abcb7* has been shown to be the cause of the ring sideroblasts. However, the key mis-spliced gene(s) that drive macrocytic anemia have not been well-determined. Mis-splicing and downregulation of *TAK1* pre-mRNA was detected in *SF3B1^{mut}*-HSPC. We found that *TAK1* is required for the survival of HSPC by restricting RIPK1-dependent and -independent PANoptosis. PANoptosis was increased in bone marrow samples from *SF3B1^{mut}*-MDS patients. To study whether *TAK1*-downregulation is the cause of anemia in *SF3B1^{mut}*-MDS, we knocked down *Tak1* (*Tak1^{KD}*) in mouse HSPC. We found that mice transplanted with *Tak1^{KD}*-HSPC developed anemia and that Ripk1 inhibition could restore blood cell counts in such anemic mice. *Tak1^{KD}*-HSPC are highly sensitive to *TAK1* inhibitor- or cIAP inhibitor-induced PANoptosis. Furthermore, RIPK1 inhibition could also correct differentiation and survival defects of *SF3B1^{mut}* human erythroblasts. *TAK1* inhibitor could also preferentially eliminate *SF3B1^{mut}* HSPC from MDS patient samples. Our study suggests that *SF3B1^{mut}* MDS can be treated by either inhibition of RIPK1-PANoptotic signaling to restore blood cell counts or activation of PANoptosis to eliminate the mutant HSPC.

Introduction

Myelodysplastic syndromes (MDS) are a heterogeneous group of preleukemic diseases which are characterized by persistent peripheral blood (PB) cytopenia, morphologic dysplasia, and a high risk of transformation to acute myeloid leukemia (AML).¹ The incidence rate of MDS is ~4.5 cases per 100,000 people annually with a median age at diagnosis of around 70 years.² The genetically mutant clonal hematopoietic stem/progenitor cells (HSPC) in MDS display defects in the generation of mature PB cells due to their

impaired differentiation and survival.³ The mutant HSPC also induce an inflammatory bone marrow (BM) microenvironment, inhibiting hematopoiesis from the remaining healthy HSPC.⁴ Furthermore, mutant HSPC exhibit a growth advantage over healthy HSPC in inflammatory BM and predispose to secondary hits which lead to transformation to AML.⁵ A better understanding of the pathogenesis of MDS and the development of novel effective targeted therapies are urgently required for these diseases.⁶ Despite showing normal to hypercellularity in BM, almost all MDS patients exhibit cytopenia due to the impaired

production of mature blood cells. Studies suggested that this ineffective hematopoiesis is caused by the aberrant activation of innate immune signaling in BM hematopoietic cells (HC) and its associated tendency toward programmed cell death (PCD) and inflammatory cytokine production.⁴ Increased apoptosis, pyroptosis and necroptosis of BM HC were reported independently by different studies to explain ineffective hematopoiesis in MDS.⁷⁻⁹ We found that all three types of PCD can be detected in individual BM tissue of most MDS patients, specifically MDS with mutations in splicing factors *SF3B1* or *SRSF2*, suggesting PANoptosis. PANoptosis is a collective term referring to all three types of PCD, pyroptosis, apoptosis and necroptosis, which can be induced by pathogen- and damage-associated molecular patterns (PAMP and DAMP) as well as combined stimulation from interferon (IFN) γ and tumor necrosis factor (TNF) α .¹⁰ It has been described recently in some pathogen infections^{11,12} and has been implicated in the pathogenesis of some chronic inflammatory diseases and cancers.^{13,14} PANoptosis is mediated by a large multi-molecular complex called a PANoptosome, containing the key signaling components of all three types of PCD (ASC/NLRP3/CASP1/11 for pyroptosis, FADD/pro-CASP8 for apoptosis, RIPK1/RIPK3 for necroptosis). The PANoptosome provides a scaffold platform for the intensive cross talk among the three PCD pathways.¹⁵ Caspase 8 (CASP8) functions as the “switch” among the three types of PCD.¹⁵ TAK1, RIPK1 and IRF1 have been described as the master regulators of PANoptosis. In many situations, RIPK1 kinase activity is required for all three types of PCD.^{11,12,15,16}

Heterozygous missense mutations of *SF3B1* have been reported in ~20% of all MDS cases, and >80% of MDS patients with ring sideroblasts (RS).¹⁷ Mutant *SF3B1* (*SF3B1^{mut}*) in HSPC primarily affects erythropoiesis which causes refractory macrocytic anemia with RS, representing a distinct nosologic entity.¹⁷ *SF3B1^{mut}* causes neomorphic function, resulting in the alternative use of cryptic splice sites of target transcripts. Aberrant splicing of a large number of transcripts has been identified in *SF3B1^{mut}* HSPC.¹⁸ Among them, mis-splicing of *Tmem14c* and *Abcb7* have been determined to be the causes of the RS phenotype.¹⁹ However, the key driver(s) for macrocytic anemia has not been identified. Mis-splicing of *TAK1* has been consistently detected in both human and mouse *SF3B1^{mut}* HSPC, resulting in nonsense-mediated decay of *TAK1* mRNA.¹⁸

To study the role of TAK1 in the pathogenesis of *SF3B1^{mut}* MDS, we knocked down *Tak1* (*Tak1^{KD}*) in HSPC using small hairpin RNA (shRNA). We found that mice which had received *Tak1^{KD}*-HSPC developed macrocytic anemia, recapitulating the phenotype observed in *Sf3b1^{+ /K700E}* mice.^{20,21} Importantly, red blood cell (RBC) counts in such anemic mice can be restored by Ripk1 inhibition. Furthermore, *Tak1^{KD}*-HSPC are hypersensitive to *Tak1* inhibitor or cIAP inhibitor treatment. Such treatments eliminate the *Tak1^{KD}*-HSPC in animal models and human *SF3B1^{mut}*-HSPC *in vitro*.

Methods

Mice

Rosa26^{CreErt}Tak1^{fx/fx} mice and *Rosa26^{CreErt}Casp8^{fx/fx}Ripk3^{-/-}* mice have been described previously. They were maintained in a C57BL/6J background.^{22,23} Wild-type (WT) C57BL/6J control mice and Ptprc recipient mice were purchased from The Jackson Laboratory (Bar Harbor, ME) and from GemPharmatech Co., Ltd. (Nanjing, China). All mice were maintained according to the standards of the National Institutes of Health Guidelines for the Care and Use of Animals in the AAALAC-certified pathogen-free animal facility at Loyola University Medical Center and at Soochow University. All mice were housed under a 12-hour light/dark cycle in microisolator cages contained within a laminar flow system. All procedures were conducted in accordance with the National Institutes of Health guidelines for the care and use of laboratory animals for research purposes and were approved in advance by the Loyola University Chicago IACUC (AU 2020-011) or the Ethics Committee of Soochow University (SUDA20221214A02, Suzhou, China). Genotypes of mice were determined by polymerase chain reaction (PCR) assay. The PCR primer sequences for genotyping can be found in *Online Supplementary Table S1*. Please see the *Online Supplementary Appendix* for more experimental procedures.

Results

Increased PANoptosis in myelodysplastic syndromes patient blood samples

To study whether PANoptosis is involved in the pathogenesis of MDS, we examined CASP3-apoptosis, NLRP3/ASC-pyroptosis and RIPK3/MLKL1-necroptosis in BM samples from 25 patients with low- to intermediate-risk MDS (15 with *SF3B1^{mut}*, 6 with *SRSF2^{mut}* and 4 without spliceosome mutations) using flow cytometry. Five BM samples from patients with iron-deficiency anemia or folic acid deficiency anemia were studied as controls. To reduce the influence of dead cells/debris generated during the process of sample collection and freezing/thawing, prior to staining, we removed the dead cells/debris by density gradient centrifugation using Ficoll-Paque™ PLUS. We believe that the cells with positive PCD markers in our analysis were dying cells with activated death signals. We found that increased apoptosis (active CASP3⁺), necroptosis (p-MLKL⁺) and pyroptosis (ASC-speck⁺) can be detected in all patient samples compared to control samples (Figure 1A, B). The PANoptosis was verified in five patients and five control samples by immunofluorescent co-staining of BM sections (Figure 1C, D). To further verify these data, we collected BM mononucleated cells (MNC) from three *SF3B1^{mut}* MDS patients to assess TAK1 protein levels and activation of PANoptotic signaling using western blotting.

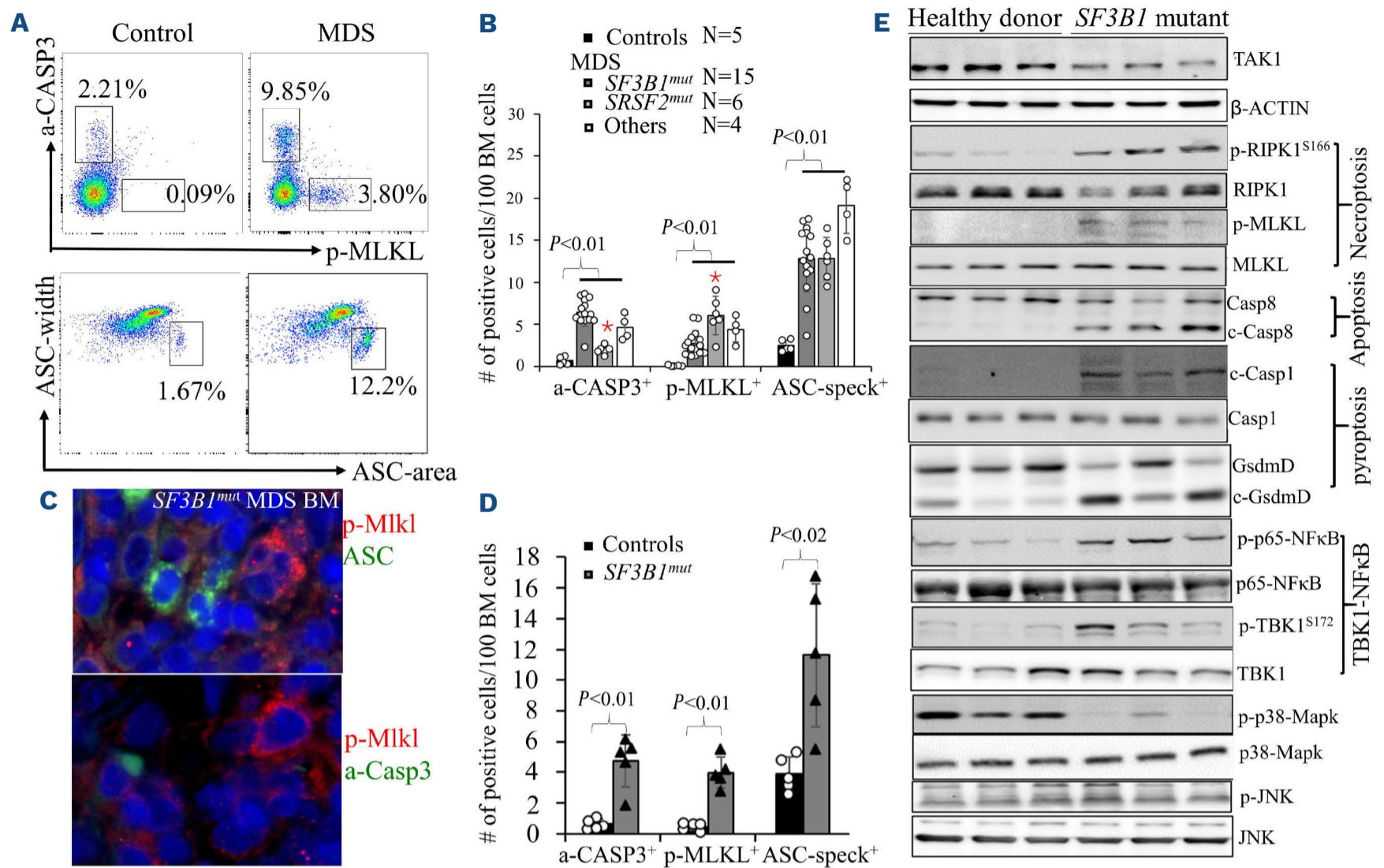


Figure 1. Increased spontaneous PANoptosis in myelodysplastic syndromes bone marrow hematopoietic cells. (A, B) Representative flow cytometric plots for p-MLKL, a(active)-CASP3 and ASC-speck analysis in myelodysplastic syndromes (MDS) and control bone marrow (BM) samples (A) and quantitated in (B). *Stands for $P < 0.05$ compared to the other 2 MDS groups. (C, D) Representative immune staining of p-MLKL, active caspase 3 (a-CASP3) and ASC-speck in MDS BM samples (C) and quantitated in (D). (E) Western blotting analysis of TAK1 and CASP8 as well as PANoptotic and TBK1-NF κ B signaling in MDS patient BM mononucleated cells (MNC) with *SF3B1* mutations compared to BM MNC from age-matched healthy donors.

Compared to BM MNC and CD34⁺ HSPC from age-matched healthy donors (HD), TAK1 levels were downregulated in all MDS patient samples (Figure 1E; *Online Supplementary Figure S1*), which are associated with increased RIPK1 activation as demonstrated by elevated p-Ser166 RIPK1. We also detected elevated apoptosis as displayed by the cleaved form of CASP8, necroptosis as shown by increased p-MLKL and pyroptosis as exhibited by cleaved forms of CASP1 and GSDMD (Figure 1E). In addition, consistent with other reported findings,²⁴ we found elevated activation of NF κ B signaling in all three MDS samples. However, p38-MAKP signaling was significantly downregulated (Figure 1E). Moreover, we found elevated activation of TBK1 signaling in all three MDS samples.

***Tak1* knockdown in hematopoietic stem/progenitor cells induces PANoptosis**

In studying *Tak1*^{-/-} mice, we and others have reported that Tak1 is required for the survival of adult HSPC. Induced deletion of *Tak1* in mice causes massive death of HSPC and acute BM failure.^{23,25} Complete depletion of hematopoietic progenitor

cells was observed 2-3 days after *Tak1* deletion while complete exhaustion of HSC occurred on days 5-6, suggesting that HSC are relatively resistant to *Tak1* deletion-induced PCD compared to HPC.^{23,26} Detailed analysis suggests that, in addition to PANoptosis, Tak1 may also protect HSPC from lysosome-mediated cell death²⁷ because PCD in *Tak1*^{-/-} HSPC can only be partially prevented by Z-VAD-FMK (pan-Casp inhibitor) + Casp8/Ripk3 depletion, which can be further prevented by the addition of the cathepsin B inhibitor CA-074Me (*Online Supplementary Figure S2*). Consistently, although BM hematopoiesis was largely normal in young *Tak1*^{-/-} *Casp8*^{-/-} *Ripk3*^{-/-} mice, increased PCD of BM HC was still detectable compared to age-matched control mice. Interestingly, Tak1 protein levels in *Tak1*^{+/-} HSPC were comparable to those in WT HSPC.^{23,26} *Tak1*^{+/-} mice were healthy and showed a normal lifespan.

To study *Tak1* expression in BM cells, we purified different stages of HSPC, committed progenitors and EB from WT mice using fluorescence-activated cell sorting (FACS) with the gating strategy described in²⁸ *Online Supplementary Figure S3A, B*. *Tak1* expression was examined by TaqMan quantitative

real-time PCR (qRT-PCR). In BM HSPC, *Tak1* expression was low in $\text{lin}^{-}\text{Sca1}^{+}\text{ckit}^{+}\text{CD150}^{+}\text{CD48}^{-}$ HSC and elevated during multipotent progenitor (MPP) and pre-GM differentiation and downregulated during further granulocyte-monocyte progenitors (GMP) and $\text{CD11b}^{+}\text{Ly6G}^{+}$ granulocyte differentiation. Highest levels of *Tak1* were detected in pre-megacaryocyte ethroid cells (pre-MegE) (Figure 2A). During the erythroid differentiation of pre-MegE, *Tak1* was downregulated in early EP pre-CFU-E and then upregulated during further differentiation of EB (Figure 2B). Aberrant splicing of 51-72% *TAK1* transcripts was detected in *SF3B1*^{mut} MDS patient cells.²⁴ To manipulate *TAK1* downregulation in *SF3B1*^{mut} HSPC, we transduced mouse HSPC using a set of three different *shRNA*, >70% reduced *Tak1* mRNA and protein levels were detected in *sh2-Tak1* and *sh3-Tak1* transductions (Figure 2C, D). Annexin-V⁺ is not specifically indicative of apoptosis; it is also positive in cells undergoing

necroptosis or pyroptosis. Compared to scrambled-*shRNA* (*Scr*)-transduced HSPC, a significant increase in spontaneous PCD was detected in HSPC transduced with *sh2-Tak1* and *sh3-Tak1* but not in HSPC transduced with *sh1-Tak1* (Online Supplementary Figure S4A). To determine the types of PCD, we transduced HSPC from WT and *Casp8*^{-/-}*Ripk3*^{-/-} mice with *sh2-Tak1* and *sh3-Tak1*. We found that the PCD of *sh2-Tak1* and *sh3-Tak1*-transduced HSPC can be partially prevented by *Casp8*^{-/-}*Ripk3*^{-/-} but is almost completely prevented by further addition of Z-VAD-FMK or VX-765 (Casp1/4 inhibitor) treatment, suggesting increased spontaneous PANoptosis of *sh2-Tak1*- and *sh3-Tak1*-HSPC (Figure 2E; Online Supplementary Figure S4B). Furthermore, PCD of *sh2-Tak1*- and *sh3-Tak1*-HSPC can be nearly completely prevented by Ripk1-specific inhibition (Figure 2E; Online Supplementary Figure S4B). However, unlike *Tak1*^{-/-} HSPC, the addition of CA-074Me failed to further prevent

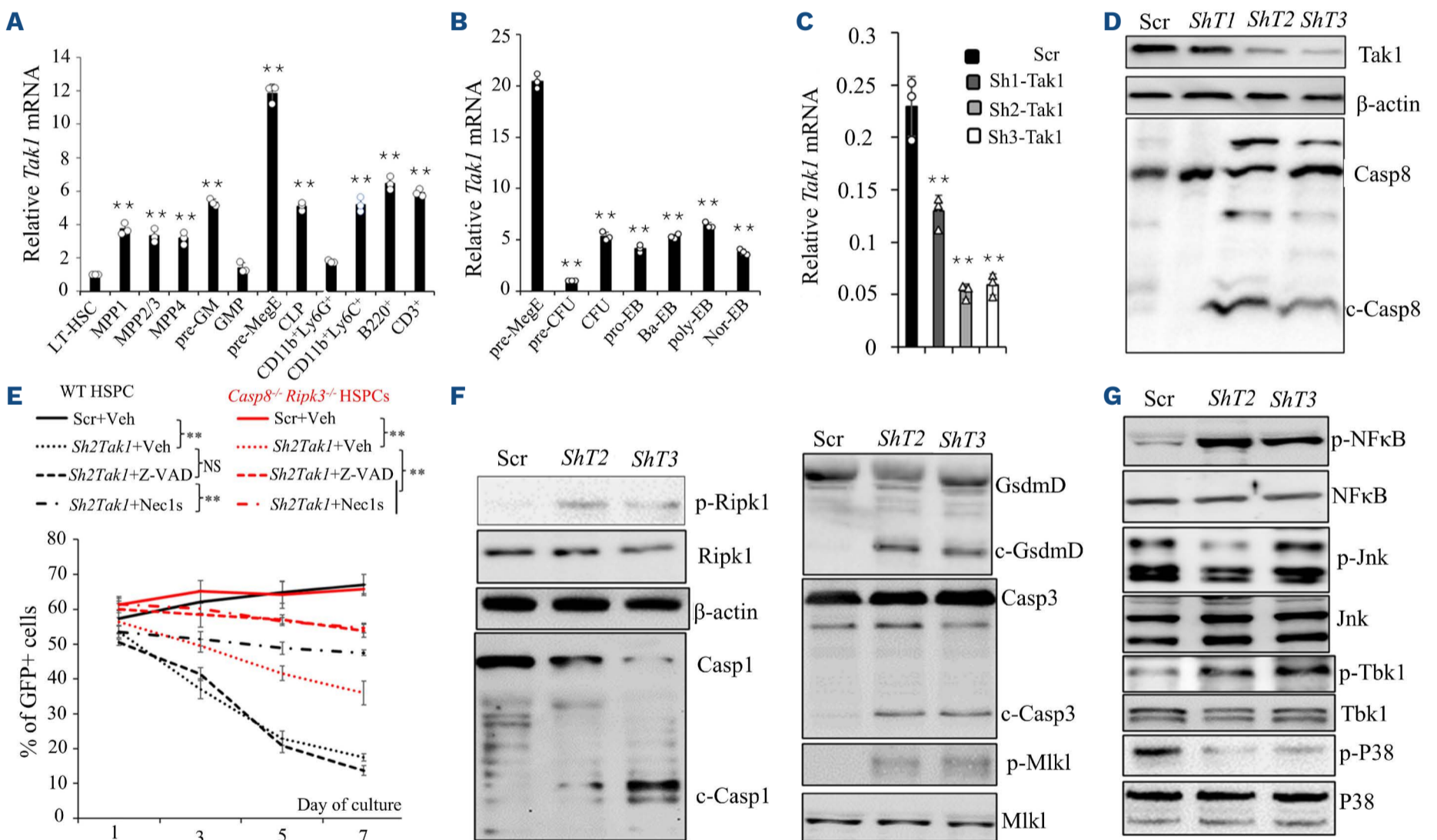


Figure 2. Increased PANoptosis in *Tak1*^{KD} hematopoietic stem/progenitor cells. (A, B) Indicated populations of hematopoietic stem progenitor cells (HSPC), erythroid precursors and erythroblasts (EB) were isolated from bone marrow (BM) of wild-type (WT) mice. *Tak1* mRNA expression was examined by quantitative real-time polymerase chain reaction (RT-PCR). Triplicate experiments were conducted. **Indicates $P < 0.01$ compared to hematopoietic stem cells (HSC) in (A) and pre-megacaryocyte erythroid cells (pre Meg-E) in (B). (C, D) c-Kit⁺ HSPC from WT mice were transduced with 3 small hairpin RNA (*shRNA*) for *Tak1*, respectively. Cells were collected on day 2 of transduction for analysis. Scrambled *shRNA* (*Scr*) transduction was studied in parallel as a control. Relative *Tak1* expression was evaluated by RT-PCR. Triplicate experiments were conducted (C). **Indicates $P < 0.01$ compared to *Scr* control. Western blot analysis of *Tak1* and *Casp8* (D). (E) c-Kit⁺ HSPC from WT and *Casp8*^{-/-}*Ripk3*^{-/-} mice were transduced with *sh2Tak1* or *Scr*. One day post-transduction, after determining the transduction efficiency (GFP⁺ cells percentage [GFP⁺%]), cells were treated with 20 μM pan-Casp inhibitor (Z-VAD) or 20 μM Ripk1 inhibitor (Nec1s) daily. The relative rate of programmed cell death (PCD) of the *Tak1*^{KD} HSPC was evaluated by detecting the GFP⁺% every 2 days. Vehicle treatments (veh) were studied in parallel as controls. Triplicate experiments were conducted. **Indicates $P < 0.01$. (F, G) c-Kit⁺ HSPC from WT mice were transduced with 2 *shRNA* for *Tak1*, respectively. Western blotting analysis of PANoptotic signaling (F), as well as Tbk1, NF κ B, Jnk and p38 signaling (G) in *shTak1* HSPC compared to *scr*-HSPC. KD: knock-down.

PCD of *sh2-Tak1*- and *sh3-Tak1*-HSPC (*Online Supplementary Figure S4C*). The PANoptosis of *sh2-Tak1* and *sh3-Tak1* HSPC was further verified by western blotting. As is the case with *SF3B1^{mut}* HSPC,¹⁸ *sh2-Tak1* and *sh3-Tak1* HSPC also displayed elevated p-Ser166 Ripk1, cleaved forms of Casp8 and Casp3, p-Mlkl and cleaved forms of Casp1 and Gsdmd (*Figure 2D, F*). *sh2-Tak1* and *sh3-Tak1* HSPC also exhibited elevated Tbk1-NFκB signaling and reduced p38-Mapk signaling (*Figure 2G*).

Mice transplanted with *Tak1^{KD}*-hematopoietic stem/progenitor cells developed myelodysplastic syndrome-like diseases

To study the role of *Tak1* in the pathogenesis of MDS, we treated *WT* C57Bl6/J mice with 10 μg lipopolysaccharide (LPS) and 125 μg polyI:C, six times each, every other day, to induce aged-related BM changes.²⁹ Two weeks post-treatment, we collected HSPC from the BM and infected with *sh3-Tak1-GFP* virus or *scr-GFP* virus. Two days post-infection, the transduced HSPC were purified by FACS for GFP⁺ cells and expanded in HSC expansion medium. The HSPC in both *sh3-Tak1*- and *scr*-groups were enriched with phenotypic HSC and comparable at the time of collection (*Online Supplementary Figure S5A*). Cells were then transplanted into lethally-irradiated mice (*Figure 3A*). We found that all mice that received *Tak1^{KD}*-HSPC developed macrocytic anemia within 3-4 months of transplantation as demonstrated by reduction of RBC counts and hemoglobin (Hb) levels as well as increased mean corpuscular volume (MCV) of red blood cells (RBC) (*Figure 3B*). In addition, these mice showed neutrocytosis as demonstrated by increased white blood cells (WBC) due to the increased CD11b⁺Ly6G⁺ neutrophils (*Figure 3B; Online Supplementary Figure S5B*); however, platelets were less affected (*Figure 3B*). Nevertheless, the BM cellularity of mice which had received *Tak1^{KD}*-HSPC was comparable to mice which had received *scr*-HSPC (*Figure 3C*). At the time of analysis, >90% of PB WBC and >80% of BM MNC were GFP⁺ in mice that had received either *Tak1^{KD}*-HSPC or *scr*-HSPC (*Online Supplementary Figure S5C*). EB lost GFP expression during maturation, explaining why GFP⁺ cell percentage (cell%) was lower in BM compared to PB. Although GFP⁺ cell% in the *Tak1^{KD}*-group tended to be reduced, there was no significant difference compared to GFP⁺ cell% in the *scr*-group. LKS⁺ (lineage⁻, c-Kit⁺ and Sca1⁺) HSPC were slightly increased in the *Tak1^{KD}*-group, while LKS⁻ (lineage⁻, c-Kit⁺ and Sca1⁻) myeloid progenitors were comparable between the two groups (*Figure 3D*). Most importantly, >98% of HSPC in both groups were GFP⁺ (*Online Supplementary Figure S5D*). HSC and GMP were increased while MPP4 and pre-MegE were reduced in the *Tak1^{KD}*-group (*Figure 3E, F; Online Supplementary Figure S5E*). However, MPP1, MPP2, MPP3, pre-GM and MkP (megakaryocyte progenitors) were comparable between the two groups (*Online Supplementary Figure S5E*). Although pre-CFU-E and CFU-E erythroid progenitors were moderately reduced in the *Tak1^{KD}*-group (*Figure 3f*), EB were increased in the BM of the *Tak1^{KD}*-group (*Figure 3G*). Within EB, the frequencies of

R2-basophilic (baso)-EB and R3-polychromatophilic (poly)-EB were reduced, while R4-orthochromatic (orth)-EB were increased (*Figure 3H*), suggesting aberrant differentiation of EB. The significantly increased PCD in c-Kit⁺ HSPC and c-Kit⁻HC, specifically in EB, suggested a critical role of PCD in the ineffective erythropoiesis (*Figure 3I*). The phenotype of *Tak1^{KD}*-mice seems to better resemble the reported phenotype of *Sf3b1^{+/K700E}* mice.^{20,21}

After anemia had developed in mice transplanted with *Tak1^{KD}*-hematopoietic stem/progenitor cells, Ripk1 inhibition mitigated this condition

To study whether the inhibition of Ripk1 can restore RBC counts in MDS mice, we transplanted another batch of mice. After moderate anemia developed (Hb <10 g/L), we randomly divided the mice into two groups. One group was treated with GNE684 (a murine Ripk1 inhibitor) twice daily for 30 days, the other group was treated with vehicle. Mice transplanted with *scr*-HSPC were studied in parallel as controls. All mice were euthanized for hematopoietic analysis 1 day after the last treatment (*Figure 4A*). We found that GNE684 treatment did not affect PB cell counts and BM hematopoiesis in mice transplanted with *scr*-HSPC (*Figure 4*). However, GNE684 treatment corrected all PB and BM hematopoietic abnormalities observed in mice transplanted with *Tak1^{KD}*-HSPC. Hb levels in vehicle-treated group were further reduced during treatment, while Hb levels in the GNE684 treatment group were significantly increased as early as 1 week of the treatment (*Figure 4B*), which were associated with correction of WBC, RBC and MCV (*Online Supplementary Figure S6A*). At 1 month of treatment, >90% of PB WBC and >80% of BM MNC in all groups of mice were GFP⁺ and comparable (*Online Supplementary Figure S6B*). PB cell counts in GNE684 treated *Tak1^{KD}*-group were restored to the levels of *scr*-controls (*Figure 4C*). In BM, the differentiation defect of EB (*Figures 4D, E*) as well as alterations of erythroid progenitors (*Figures 4F*) and HSPC (*Figures 4G; Online Supplementary S6C, D*) were largely corrected in the GNE684-treated group. The increased PCD of HC, HSPC and EB was inhibited in the GNE684-treated group (*Figure 4H*).

To study whether the premature differentiation of *Tak1^{KD}*-EB is related to premature downregulation of Gata1 as described in *SF3B1^{mut}*-EB,²⁴ we cultured *Tak1^{KD}*- and *scr*-HSPC in a two-phase *in vitro* erythropoiesis system. After 6 days of expansion, the cells were transferred into differentiation medium for further incubation. Cells were collected after 12, 24 and 48 hours of culturing for analysis. We found that Gata1 was downregulated as early as 24 hours in *Tak1^{KD}*-EB, which was significantly earlier than Gata1 downregulation in *scr*-EB (*Online Supplementary Figure S6E*). However, the differentiation stages of *Tak1^{KD}*-EB at 24 hours of culture were comparable to those of *scr*-EB (*Online Supplementary Figure S6F*), suggesting premature Gata1 downregulation. The premature downregulation of Gata1 could be prevented by Ripk1 inhibition, and Ripk3/Casp8 inhibition (*Online Supplementary Figure S6G*),

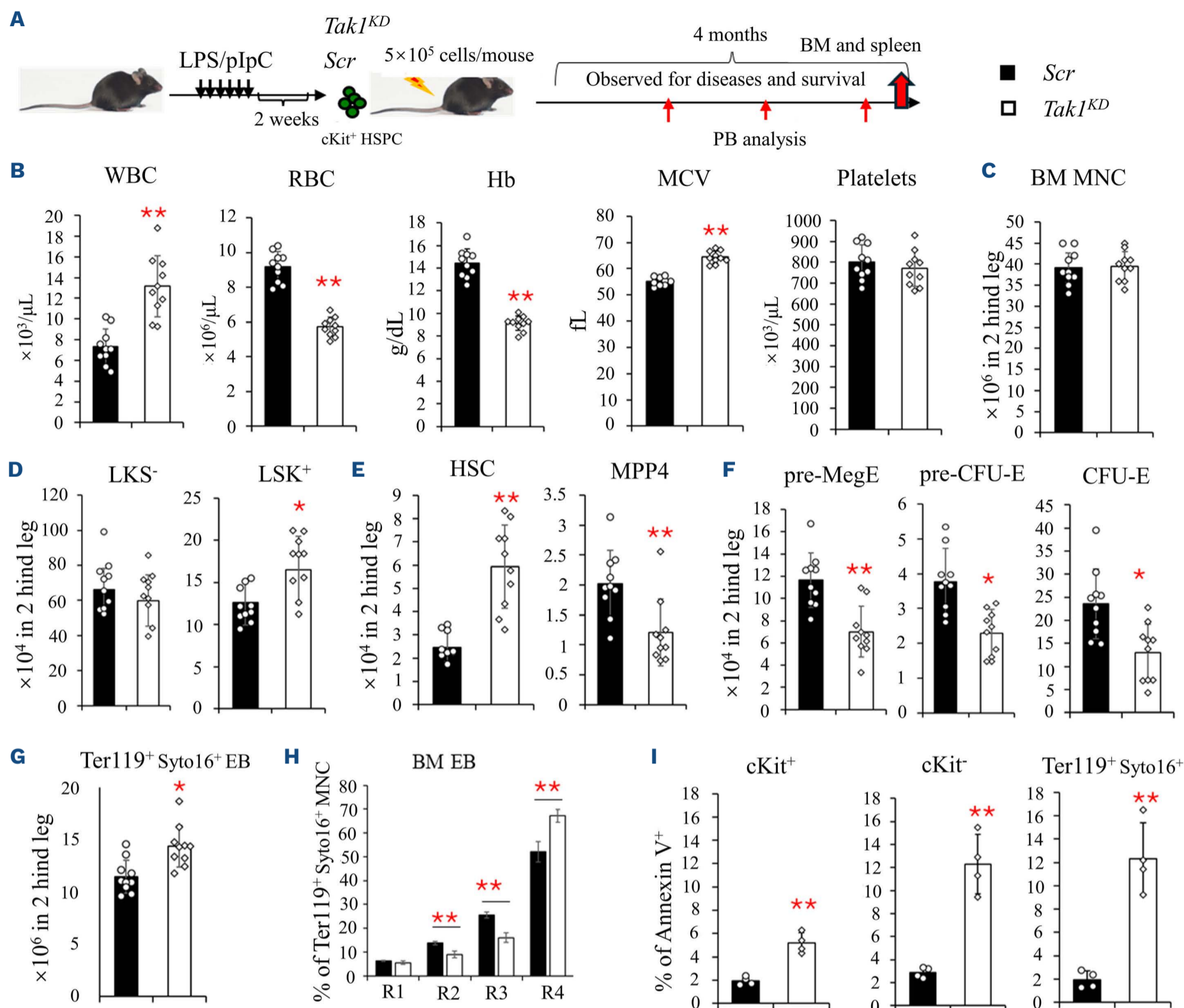


Figure 3. Mice transplanted with *Tak1*^{KD} hematopoietic stem/progenitor cells developed myelodysplastic syndrome-like diseases. (A) Schematic diagram of experimental procedures. Four months post-transplantation of scrambled small hairpin hematopoietic stem/progenitor cells (*scr*-HSPC) and *Tak1*^{KD} HSPC, peripheral blood (PB) cell counts were examined using a Hemavet (B). (C-I) Bone marrow (BM) was collected, and mononucleated cells (MNC) (C), LKS⁻ myeloid progenitors and LSK⁺ HSPC (D), hematopoietic stem cell (HSC) and MPP4 (E), pre-megacaryocyte erythroid cells (pre-MegE), pre-colony forming unit erythroid cells (pre-CFU-E) and CFU-E (F), as well as erythroblasts (EB) including R1-pro-EB, R2-basophilic (baso)-EB, R3-polychromatophilic (poly)-EB and R4-orthochromatic (ortho)-EB (G, H) were analyzed by flow cytometry. Programmed cell death (PCD) of cKit⁺ HSPC, cKit⁻ hematopoietic cells (HC) and Syto16⁺Ter119⁺ EB were analyzed by flow cytometry for Annexin-V staining (I). KD: knock-down.

suggesting a Ripk1-Ripk3/Casp8-dependent mechanism of Gata1 downregulation. In addition, the elevated NF κ B signaling in *Tak1*^{KD}-HSPC can also be repressed by Ripk1 inhibition and Tbk1 inhibition, implicating a Ripk1-Tbk1 axis-mediated NF κ B activation (*Online Supplementary Figure S6H*).

***Tak1*^{KD}-hematopoietic stem/progenitor cells are sensitive to *Tak1* inhibitor and cIAP inhibitor treatment**

We speculate that *Tak1*^{KD}-HSPC rely on residual *Tak1* activity

for their survival, and *Tak1* inhibition might induce synthetic lethality in *Tak1*^{KD}-HSPC. We treated *Tak1*^{KD}-HSPC and *scr*-HSPC with the cIAP inhibitor birinapant or the *Tak1* inhibitor HS-276. In mixed suspension culture of transduced and no-transduced HSPC (Figure 5A), both birinapant and HS-276 preferentially killed *Tak1*^{KD}-HSPC with reduced effect on *scr*-HSPC as demonstrated by significantly reduced percentage of *Tak1*^{KD}-HSPC (Figure 5B). In methylcellulose clonal assays, both birinapant and HS-276 treatment yielded significantly

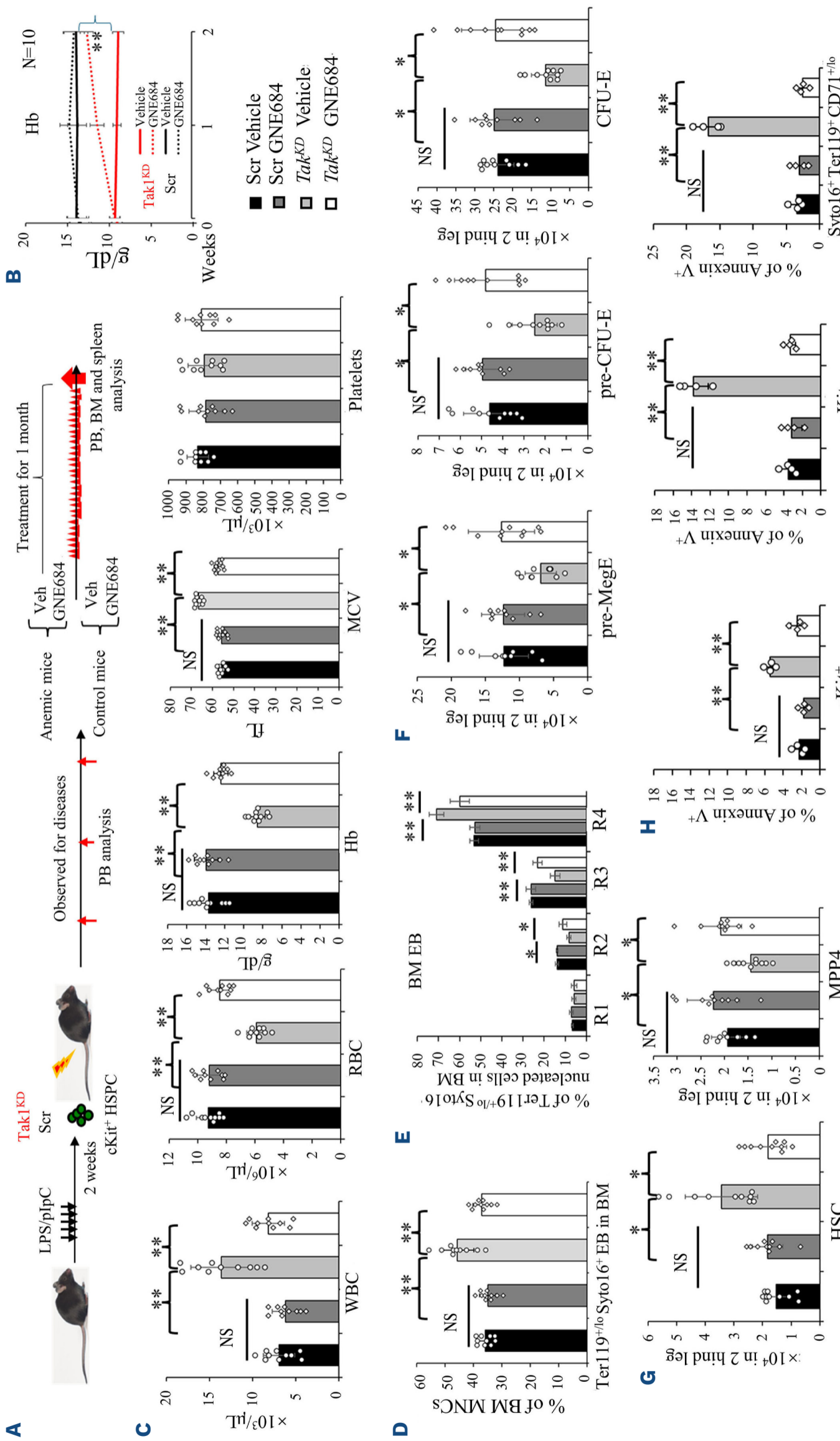


Figure 4. Ripk1 inhibition restores normal bone marrow hematopoiesis and blood cell counts in anemic *Tak1*^{KD} mice. (A) Schematic diagram of experimental procedures. (B-G) After anemia developed (hemoglobin [Hb] <10 g/dL), the mice were randomly separated into 2 groups and treated with vehicle or GNE684, respectively, for 1 month. Scrambled small hairpin RNA hematopoietic stem/progenitor cell (scr-HSPC) transplantations were studied in parallel as controls. Peripheral blood (PB) Hb levels were analyzed on 1 day before treatment (0) as well as at 1 and 2 weeks during the treatment (B). The percentages of erythroblasts (EB) (D) and different differentiation stages of EB in bone marrow (BM) (E), absolute numbers of pre-megacaryocyte erythroid cells (pre-MegE) and erythroid progenitors (EP) (F), and absolute numbers of hematopoietic stem cells (HSC) and MPP4 (G) in BM were analyzed by flow cytometry. The percentages of programmed cell death (PCD) of c-Kit⁻ hematopoietic cells (HC), c-Kit⁺ HSPC and Syto16⁺/Ter119⁺ EB were examined by flow cytometric analysis of Annexin-V staining (H). NS: not significant; * and ** indicate $P < 0.05$ and $P < 0.01$, respectively; KD: knock-down.

reduced clone-forming ability of *Tak1^{KD}*-HSPC with reduced effect on *scr*-HSPC (Figure 5c). To study inhibition of Tak1 signaling on *Tak1^{KD}*-HSPC *in vivo*, we transplanted a mixture of *Tak1^{KD}*-HSPC and normal HSPC into recipient mice. Thirty days after transplantation and following an examination of

the percentages of PB contributions of *Tak1^{KD}*-HSPC, the recipient mice were randomly divided into three groups. Mice in groups 1 and 2 were treated with HS-276 and birinapant, respectively, while mice in group 3 were treated with vehicle (Figure 5a). We found that HS-276 and birinapant treatment

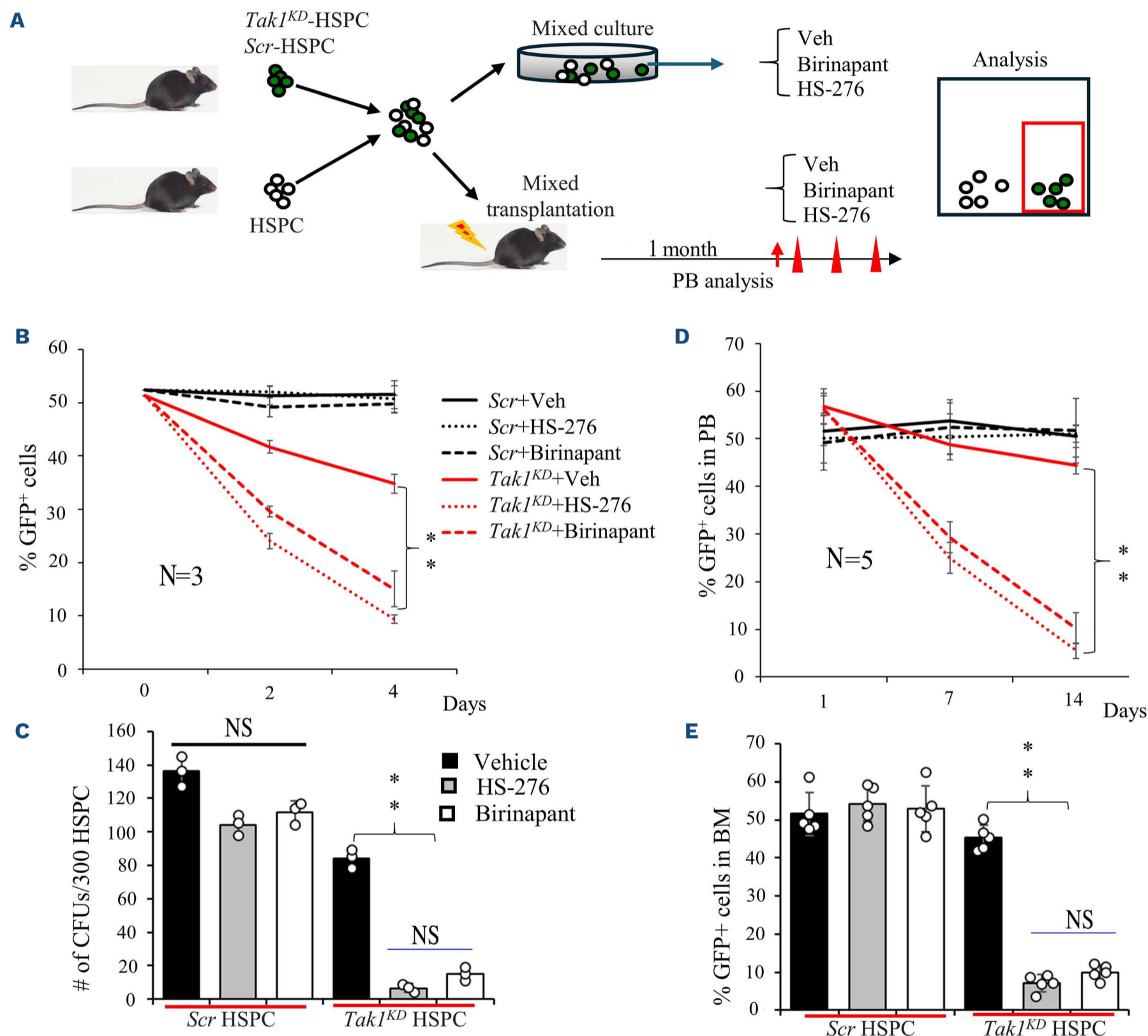


Figure 5. *Tak1* inhibitor or cIAP-inhibitor treatment induces synthetic lethality in *Tak1^{KD}* hematopoietic stem/progenitor cells. (A) Schematic diagram of experimental procedures. (B) Small hairpin (*sh*)2*Tak1*-GFP-transduced hematopoietic stem/progenitor cells (HSPC) (*Tak1^{KD}*) were mixed with untransduced HSPC in a 1:1 ratio and treated with vehicle (Veh), *Tak1* inhibitor HS-276 or cIAP-inhibitor birinapant. New chemicals were added on day 2 during medium change. The reduction of the transduced HSPC was examined by analyzing the GFP⁺ cell percentage. Scrambled RNA (*scr*)-GFP transduced HSPC were studied in parallel as controls. (C) *Tak1^{KD}* - and *scr*-transduced HSPC were seeded for colony-forming unit (CFU) assay and treated with vehicle, HS-276 or birinapant. CFU numbers were counted on day 7 of culturing. Three biological replicates were performed for data in (B) and (C). (D, E) *Tak1^{KD}* HSPC (GFP⁺) were mixed with non-transduced HSPC in a 1.5:1 ratio, whereas *scr*-GFP transduced HSPC were mixed with non-transduced HSPC in a 1:1 ratio. The mixed HSPC were transplanted into lethally-irradiated mice. One month post-transplantation, after determining the engraftment (GFP⁺ cells in peripheral blood [PB]) of the transduced HSPC, mice were divided into 3 groups and treated with vehicle, HS-276 or birinapant, respectively, for 2 weeks. The percentages of transduced cells in PB (D) were examined on days 7 and 14, and in bone marrow (BM) were examined on day 14 (E). KD: knock-down; **indicates *P* < 0.01; NS: not significant.

did not affect the PB and BM contributions of *scr*-HSPC but largely eliminated the *Tak1^{KD}*-HSPC-derived cells in the recipient animals as demonstrated by a significant reduction of GFP⁺ percentage in PB and BM (Figure 5D, E). When analyzed 2 months after HS-276 and birinapant withdrawal, blood cell counts in HS-276 and birinapant-treated groups remained normal (Online Supplementary Figure S7A) and were primarily replenished by GFP⁻ normal HSPC (Online Supplementary Figure S7B). However, the RBC counts and Hb levels in the vehicle-treated mice were slightly lower than in control group mice (Online Supplementary Figure S7A).

RIPK1 inhibition restored the proper growth of *SF3B1^{mut}*-erythroblasts from myelodysplastic patients

SF3B1^{mut}-MDS HSPC displayed a reduced clone-forming ability and a late erythroid differentiation defect^{24,30} (Figure 6A). We seeded BM MNC from *SF3B1^{mut}*-MDS patients for colony-forming unit (CFU) assay with or without RIPK1 inhibitor GSK3145095 treatment. We found that GSK3145095 did not affect the colony-forming capacity of HSPC from HD but increased colony-forming capacity of *SF3B1^{mut}*-MDS HSPC (Figure 6A). To study whether inhibition of RIPK1 can restore survival and normal differentiation to *SF3B1^{mut}*-HSPC, we isolated CD34⁺ HSPC from BM of MDS patients and HD. Using the three-phase erythroid culture system with medium change every-other day³¹ (Figure 6B), GSK3145095 or vehicle were added during medium changes. Compared to HSPC from five HD, HSPC from all five MDS samples produced significantly fewer cells during 14 days of culturing (Figure 6C). Although comparable numbers of BFU-E and CFU-E were produced by MDS-HSPC and HD-HSPC by day 7 of expansion culture, a significant reduction of Pro-EB was observed in the MDS culture (Figure 6D; Online Supplementary Figure S8A). When examined on day 14, a significantly reduced number of late-baso-EB, poly-EB, ortho-EB and reticulocytes (Ret) was detected in MDS culture (Figure 6E, F; Online Supplementary Figure S8A, B).³² GSK3145095 treatment affected neither the expansion of BFU-E/CFU-E nor the differentiation of HD-EB; however, GSK3145095 treatment significantly enhanced the production of EB and Ret of MDS-HSPC (Figure 6C-F). The reduced production of EB and Ret of MDS-HSPC was most likely due to the increased RIPK1-dependent PCD and late differentiation blockage because both can be largely reversed by GSK3145095 treatment (Figure 6E, G).

Tak1 inhibitor treatment preferentially killed *SF3B1^{mut}*-hematopoietic stem/progenitor cells

To study whether TAK1 inhibitor treatment can induce synthetic lethality in *SF3B1^{mut}*-HSPC, we isolated CD34⁺ HSPC from MDS patients and HD. The HSPC were incubated in Soluplus-based 4a-HSPC expansion medium and treated with 10 μM HS-276. Cells were collected on day 3 of culturing for RIPK1 and p-RIPK1 protein level analysis, on day 4 for cell death analysis, and on day 6 for live-cell counts

and targeted DNA-sequencing to detect mutational variant allele frequency (VAF) of the *SF3B1^{mut}* genes (Figure 6H). In the vehicle-groups, p-RIPK1 levels and cell death were higher in MDS HSPC compared to HD HSPC (Figures 6I; Online Supplementary Figure S9A, B). HS276 treatment tended to induce p-RIPK1 in HD HSPC but triggers much higher p-RIPK1 levels in MDS HSPC (Figure 6I; Online Supplementary Figure S9A). Consistently, we found a more significant increase in PCD in MDS HSPC compared to HD-HSPC after HS276 treatment (Figures 6J; Online Supplementary Figure S9B) which resulted in a significant reduction of live cells in MDS samples (Online Supplementary Figure S9C). VAF analysis of mutant genes demonstrated that HS-276 treatment significantly reduced *SF3B1^{mut}*-HSPC (Figure 6k).

Discussion

Increased PCD and blockage of terminal erythroid differentiation of EB are believed to be the major causes of ineffective erythropoiesis observed in *SF3B1^{mut}*-MDS patients.^{17,33} Mis-splicing of TAK1 is always detected in *SF3B1^{mut}* cells, which leads to nonsense decay of *TAK1* mRNA.^{18,24} Our study suggests that TAK1 downregulation is the major cause of ineffective erythropoiesis in *SF3B1^{mut}*-MDS patients. We found TAK1-downregulation and increased spontaneous PANoptosis in BM samples of *SF3B1^{mut}*-MDS patients. *Tak1*-downregulation results in Ripk1 overactivation and spontaneous PANoptosis in mouse HSPC. In both murine *Tak1^{KD}*-HSPC and human *SF3B1^{mut}*-HSPC, the inhibition of RIPK1 can prevent PANoptosis and correct the differentiation defects of EB. Furthermore, both human *SF3B1^{mut}*-HSPC and murine *Tak1^{KD}*-HSPC are hypersensitive to the inhibition of TAK1 signaling. Our study suggests that *SF3B1^{mut}*-MDS can be treated by either inhibition of RIPK1-PANoptosis to restore normal erythropoiesis or by inhibition of TAK1 signaling to induce synthetic lethality of the mutant HSPC.

RIPK1 overactivation not only promotes spontaneous PANoptosis of EB but also induces aberrant differentiation of EB. Consistent with the findings of Lieu et al.,²⁴ we found that the aberrant differentiation of *Tak1^{KD}*-EB is associated with premature downregulation of Gata1. Lieu et al. proposed that TAK1 downregulation promotes the proteasomal degradation of GATA1 via the p38-MK2/HSP27 pathway.^{24,34} In fact, downregulation of p38-MK2 signaling can also cause RIPK1 activation.^{35,36} We found that the premature downregulation of Gata1 in *Tak1^{KD}*-EB is largely mediated by Ripk1-Casp8 signaling. Although Casp8 cannot directly cleave Gata1, it activates Casp3 and Casp1, both of which can cleave Gata1.^{37,38} Thus, both spontaneous PANoptosis and the premature differentiation defects of *Tak1^{KD}*- or *Sf3b1^{+/K700E}*-EB can be reversed by Ripk1 inhibition. Many RIPK1-specific inhibitors have been developed. Several of them have been evaluated in clinical trials for autoimmune

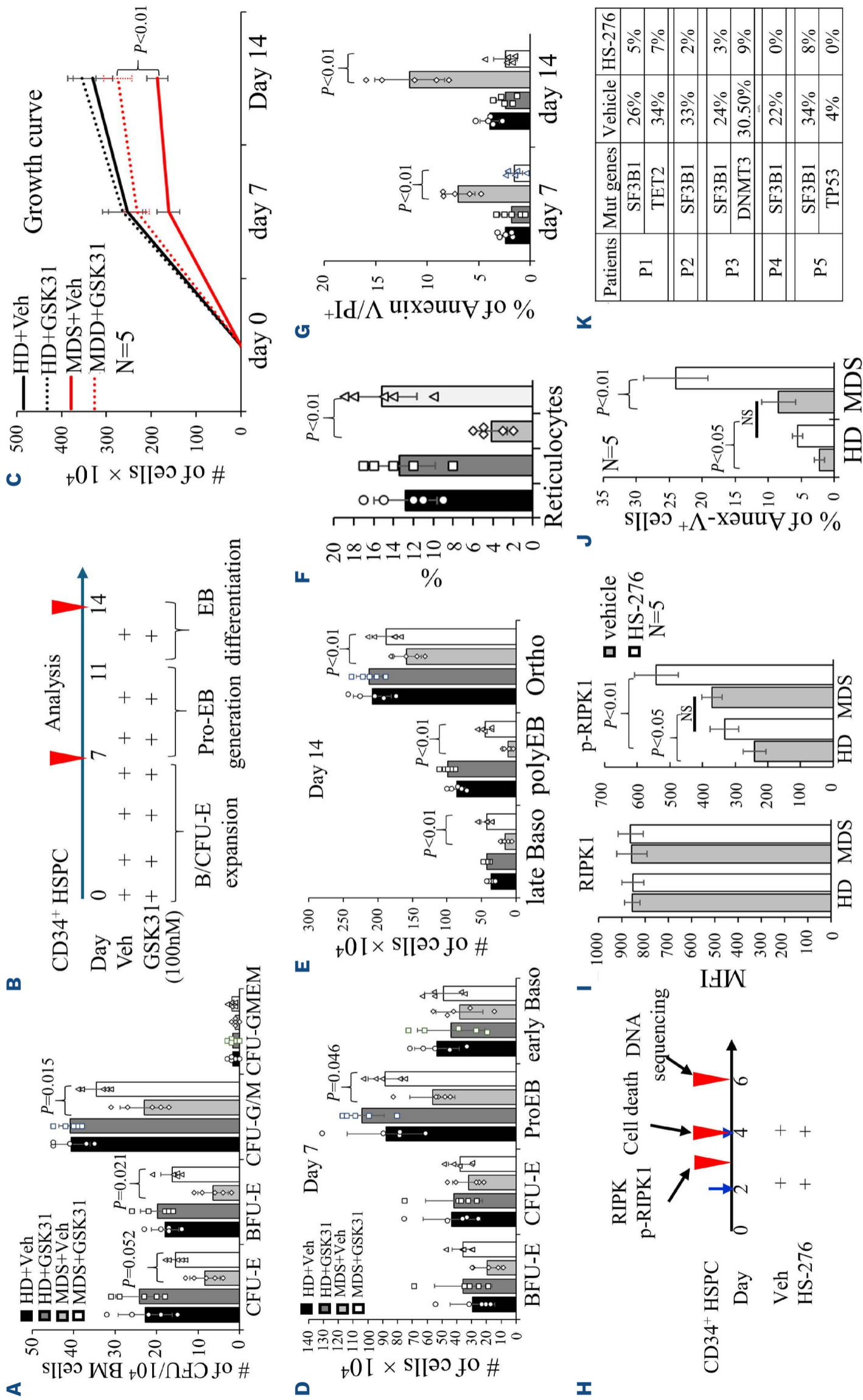


Figure 6. Inhibition of RIPK1 and TAK1 in human SF3B1^{mut} myelodysplastic syndromes samples. (A) Bone marrow (BM) cells from myelodysplastic syndromes (MDS) patients and healthy donors (HD) were seeded into M3343 medium for colony-forming unit (CFU) assay with or without RIPK1 inhibitor GSK3145095 treatment. CFU-erythroid cells (CFU-E) were counted on day 7 of culturing and BFU-E, CFU-granulocytes/megacaryocytes (GM) and CFU-GMEM were counted on day 14 of culturing. (B) Schematic diagram of experimental procedures for (C-G) CD34⁺ hematopoietic stem/progenitor cells (HSPC) from HD or MDS patients were cultured in 3-phase erythroid culture system with or without GSK3145095 treatment. Cells were collected on days 7 and 14 of culturing; the numbers of cultured cells were plotted in the growth curve (C); BFU-E, CFU-E, pro-erythroblasts (pro-EB) and early basophilic EB (baso-EB) were analyzed by flow cytometry on day 7 (D); late baso-EB, polychromatophilic (poly)-EB and orthochromatic (ortho)-EB (e) and reticulocytes (Ret) were analyzed by flow cytometry on day 14. Programmed cell death (PCD) was analyzed on days 7 and 14, respectively, by examining Annexin-V⁺ cells (G). (H) Schematic diagram of experimental procedure for (I-K). CD34⁺ HSPC from HD or MDS patients were cultured in HSPC culture system with or without TAK1 inhibitor HS-276 treatment. Cells were collected on day 3 of culturing for analysis of RIPK1 and p-RIPK1 protein level by flow cytometry (I), day 4 for cell death analysis by Annexin-V/propidium iodide (PI) staining (J), and day 6 for targeted DNA sequencing (K). Mean fluorescence intensity (MFI) of RIPK1 and p-RIPK1 staining (I), and percentage of Annexin-V⁺ cells (J) were presented. The variant allele frequency of mutant genes are presented in the Table (K). NS: not significant.

and neuroinflammatory diseases, and have shown excellent safety and promising results.³⁹ Therefore, it will be important to test whether RIPK1 inhibition can mitigate the anemia that is so common in *SF3B1^{mut}*-MDS patients.

In normal HC, PANoptosis is restricted by TAK1 signaling. TAK1 signaling is normally activated by PAMP, DAMP and inflammatory cytokines.^{40,41} TAK1 and its downstream signaling mediators IKK/NEMO and MK2 limit RIPK1-dependent PANoptosis by phosphorylating RIPK1.³⁹ cIAP1/2 and LUBAC, the upstream mediators of TAK1 signaling, also repress RIPK1-dependent PANoptosis by mediating K63- and M1-linked ubiquitination of RIPK1.⁴² In BM-derived macrophages (BMDM), *Tak1*^{-/-} induces spontaneous Ripk1-dependent PANoptosis.⁴³ TAK1 signaling also restricts RIPK1-independent PANoptosis by regulating NFκB-mediated the expression of several pro-survival genes. BMDM deficient in *Tak1* are hypersensitive to LPS or polyI:C-induced Ripk1-dependent and -independent PANoptosis.⁴⁴ However, all of our experiments were performed in a specific pathogen-free environment without any PAMP challenges. Future study needs to determine whether Ripk1 inhibitor treatment can also mitigate anemia in mice with *Tak1^{KD}*-HSPC or *Sf3b1^{+/-K700E}*-HSPC in a pathogen infection setting. In addition, we used LPS/polyI:C pre-treated BM HSPC in our transduction studies. Although LPS/polyI:C pre-treatment only induces age-like epigenetic/metabolic memory in BM HSPC without increasing genetic mutations,²⁹ it is not known whether *Tak1^{KD}* in HSPC from untreated young or old mice can also induce MDS-like disease. Furthermore, future study needs to elucidate why *Tak1^{KD}* in HSPC primarily affects certain stages of EB.

In most types of tissue cells, TAK1 inactivation is always associated with NFκB signaling inhibition.⁴⁰ However, in *SF3B1^{mut}*-HSPC, NFκB signaling activity is enhanced.¹⁸ We found that such TAK1-independent NFκB signaling activation is most likely due to the overactivation of RIPK1-TBK1 signaling. In addition to activating PANoptosis, activated RIPK1 can also activate TBK1-dependent IFNα/β^{22,45} and NFκB signaling.⁴⁶ Activated RIPK1 can also translocate to the nucleus to promote the expression of *NFκB* target genes by recruiting a BAF complex to enhancers/promoters.⁴⁷ Therefore, active RIPK1 might promote NFκB signaling activity via both TBK1-mediated regulation and BAF complex-mediated tight gene expression.

We found that TAK1 is downregulated in BM HC from patients with *SF3B1^{mut}*-MDS, while dysregulation of other master regulators of the PANoptotic pathway have been reported in MDS patients with other genetic mutations. For example, mutations of *SRSF2* cause mis-splicing of *CASP8*.¹⁸ Down-regulating *CASP8* results in hypersensitivity of cells to necroptosis and pyroptosis due to elevated RIPK1 protein levels.¹⁵ In low-grade MDS patients, downregulation of *CASP8* and increased RIPK1 protein are detected in BM HC.⁴⁸ *Ripk1*

overexpression or *Casp8* knockout in HSPC induces PCD and MDS-like disease in mice.^{9,22} Thus, targeting PANoptotic signaling might also be a useful strategy for treating MDS with other genetic mutations.

Although increased PCD is commonly detected in HC from MDS patients, the number of HSPC in MDS patients is not reduced, most likely due to inflammatory cytokine-stimulated compensatory proliferation. Cells which die of PANoptosis produce inflammatory cytokines such as TNFα and IL1β. TNFα and IL1β induce PCD and differentiation in myeloid progenitor cells.^{49,50} However, owing to the higher-level expression of pro-survival genes such as cIAP2, HSC are relatively resistant to inflammatory cytokine-induced PCD.⁴⁹ Currently, we are developing more sensitive assays for the detection of PANoptosis. We want to determine which cell populations in MDS patient BM are undergoing PANoptosis. We also want to distinguish whether all three types of PCD occur in the same cells *versus* different cell types.

Disclosures

No conflicts of interest to disclose.

Contributions

LZ, WL and JWZ designed the experiments, analyzed the data, and drafted the manuscript. JWZ supervised the overall research, designed the experiments, analyzed the data, and edited the manuscript; LZ, WL, RT, RYM, RM, AK, AR, PH, KB, JKS, JK, PB, HLJ, and JWZ collectively contributed to data collection and interpretation of the results. AK, PH, KB and JKS provided study samples, clinical data, and helped to revise the manuscript. PB and JWZ helped to write and also edited and refined the manuscript.

Acknowledgments

The authors thank the staff of the Department of Comparative Medicine at Loyola University Medical Center for their excellent animal care services, as well as Ms. Patricia Simms for flow cytometric sorting of HSC and progenitors.

Funding

This work was supported by NIH grants NHLBI R01 HL133560, NCI R01 CA223194 and NCI R01 CA301049 through Loyola University Chicago as well as by Loyola Program Development funding to JWZ. It was also supported by Interdisciplinary Basic Frontier Innovation Program of Suzhou Medical College of Soochow University (YXY2304063), and the Priority Academic Program Development of Jiangsu Higher Education Institutions (PAPD) to JZ.

Data-sharing statement

Original data, protocols and reagents are available to other investigators upon request.

References

1. Sekeres MA, Taylor J. Diagnosis and treatment of myelodysplastic syndromes: a review. *JAMA*. 2022;328(9):872-880.
2. McQuilten ZK, Wood EM, Polizzotto MN, et al. Underestimation of myelodysplastic syndrome incidence by cancer registries: results from a population-based data linkage study. *Cancer*. 2014;120(11):1686-1694.
3. Nazha A, Sekeres MA, Bejar R, et al. Genomic biomarkers to predict resistance to hypomethylating agents in patients with myelodysplastic syndromes using artificial intelligence. *JCO Precis Oncol*. 2019;3:PO.19.00119.
4. Sallman DA, List A. The central role of inflammatory signaling in the pathogenesis of myelodysplastic syndromes. *Blood*. 2019;133(10):1039-1048.
5. Vallelonga V, Gandolfi F, Ficara F, et al. Emerging insights into molecular mechanisms of inflammation in myelodysplastic syndromes. *Biomedicines*. 2023;11(10):2613.
6. Steensma DP. Graphical representation of clinical outcomes for patients with myelodysplastic syndromes. *Leuk Lymphoma*. 2016;57(1):17-20.
7. Parker JE, Mufti GJ, Rasool F, et al. The role of apoptosis, proliferation, and the Bcl-2-related proteins in the myelodysplastic syndromes and acute myeloid leukemia secondary to MDS. *Blood*. 2000;96(12):3932-3938.
8. Basiorka AA, McGraw KL, Eksioglu EA, et al. The NLRP3 inflammasome functions as a driver of the myelodysplastic syndrome phenotype. *Blood*. 2016;128(25):2960-2975.
9. Wagner PN, Shi Q, Salisbury-Ruf CT, et al. Increased Ripk1-mediated bone marrow necroptosis leads to myelodysplasia and bone marrow failure in mice. *Blood*. 2019;133(2):107-120.
10. Sharma BR, Karki R, Rajesh Y, et al. Immune regulator IRF1 contributes to ZBP1-, AIM2-, RIPK1-, and NLRP12-PANoptosome activation and inflammatory cell death (PANoptosis). *J Biol Chem*. 2023;299(9):105141.
11. Sundaram B, Pandian N, Mall R, et al. NLRP12-PANoptosome activates PANoptosis and pathology in response to heme and PAMP. *Cell*. 2023;186(13):2783-2801.e2720.
12. Lee S, Karki R, Wang Y, et al. AIM2 forms a complex with pyrin and ZBP1 to drive PANoptosis and host defence. *Nature*. 2021;597(7876):415-419.
13. Qi Z, Zhu L, Wang K, et al. PANoptosis: emerging mechanisms and disease implications. *Life Sci*. 2023;333:122158.
14. Cai H, Lv M, Wang T. PANoptosis in cancer, the triangle of cell death. *Cancer Med*. 2023;12(24):22206-22223.
15. Christgen S, Zheng M, Kesavardhana S, et al. Identification of the PANoptosome: a molecular platform triggering pyroptosis, apoptosis, and necroptosis (PANoptosis). *Front Cell Infect Microbiol*. 2020;10:237.
16. Malireddi RKS, Kesavardhana S, Kanneganti TD. ZBP1 and TAK1: master regulators of NLRP3 inflammasome/pyroptosis, apoptosis, and necroptosis (PAN-optosis). *Front Cell Infect Microbiol*. 2019;9:406.
17. Malcovati L, Stevenson K, Papaemmanuil E, et al. SF3B1-mutant MDS as a distinct disease subtype: a proposal from the International Working Group for the Prognosis of MDS. *Blood*. 2020;136(2):157-170.
18. Lee SC, North K, Kim E, et al. Synthetic lethal and convergent biological effects of cancer-associated spliceosomal gene mutations. *Cancer Cell*. 2018;34(2):225-241.e228.
19. Clough CA, Pangallo J, Sarchi M, et al. Coordinated missplicing of TMEM14C and ABCB7 causes ring sideroblast formation in SF3B1-mutant myelodysplastic syndrome. *Blood*. 2022;139(13):2038-2049.
20. Mupo A, Seiler M, Sathiaselvan V, et al. Hemopoietic-specific Sf3b1-K700E knock-in mice display the splicing defect seen in human MDS but develop anemia without ring sideroblasts. *Leukemia*. 2017;31(3):720-727.
21. Obeng EA, Chappell RJ, Seiler M, et al. Physiologic expression of Sf3b1(K700E) causes impaired erythropoiesis, aberrant splicing, and sensitivity to therapeutic spliceosome modulation. *Cancer Cell*. 2016;30(3):404-417.
22. Liu S, Joshi K, Zhang L, et al. Caspase 8 deletion causes infection/inflammation-induced bone marrow failure and MDS-like disease in mice. *Cell Death Dis*. 2024;15(4):278.
23. Tang M, Wei X, Guo Y, et al. TAK1 is required for the survival of hematopoietic cells and hepatocytes in mice. *J Exp Med*. 2008;205(7):1611-1619.
24. Lieu YK, Liu Z, Ali AM, et al. SF3B1 mutant-induced missplicing of MAP3K7 causes anemia in myelodysplastic syndromes. *Proc Natl Acad Sci U S A*. 2022;119(1):e2111703119.
25. Takaesu G, Inagaki M, Takubo K, et al. TAK1 (MAP3K7) signaling regulates hematopoietic stem cells through TNF-dependent and -independent mechanisms. *PLoS One*. 2012;7(11):e51073.
26. Xiao Y, Li H, Zhang J, et al. TNF-alpha/Fas-RIP-1-induced cell death signaling separates murine hematopoietic stem cells/progenitors into 2 distinct populations. *Blood*. 2011;118(23):6057-6067.
27. Sakamachi Y, Morioka S, Mihaly SR, et al. TAK1 regulates resident macrophages by protecting lysosomal integrity. *Cell Death Dis*. 2017;8(2):e2598.
28. Liu J, Zhang J, Ginzburg Y, et al. Quantitative analysis of murine terminal erythroid differentiation in vivo: novel method to study normal and disordered erythropoiesis. *Blood*. 2013;121(8):e43-49.
29. Yokomizo-Nakano T, Hamashima A, Kubota S, et al. Exposure to microbial products followed by loss of Tet2 promotes myelodysplastic syndrome via remodeling HSCs. *J Exp Med*. 2023;220(7):e20220962.
30. DeZern AE, Pu J, McDevitt MA, et al. Burst-forming unit-erythroid assays to distinguish cellular bone marrow failure disorders. *Exp Hematol*. 2013;41(9):808-816.
31. Hu J, Liu J, Xue F, et al. Isolation and functional characterization of human erythroblasts at distinct stages: implications for understanding of normal and disordered erythropoiesis in vivo. *Blood*. 2013;121(16):3246-3253.
32. Yan H, Ali A, Blanc L, et al. Comprehensive phenotyping of erythropoiesis in human bone marrow: evaluation of normal and ineffective erythropoiesis. *Am J Hematol*. 2021;96(9):1064-1076.
33. Fenaux P, Platzbecker U, Mufti GJ, et al. Luspatercept in patients with lower-risk myelodysplastic syndromes. *N Engl J Med*. 2020;382(2):140-151.
34. de Thonel A, Vandekerckhove J, Lanneau D, et al. HSP27 controls GATA-1 protein level during erythroid cell differentiation. *Blood*. 2010;116(1):85-96.
35. Dondelinger Y, Delanghe T, Rojas-Rivera D, et al. MK2 phosphorylation of RIPK1 regulates TNF-mediated cell death. *Nat Cell Biol*. 2017;19(10):1237-1247.
36. Menon MB, Gropengiesser J, Fischer J, et al. p38(MAPK)/MK2-dependent phosphorylation controls cytotoxic RIPK1 signalling

- in inflammation and infection. *Nat Cell Biol.* 2017;19(10):1248-1259.
37. Tyrkalska SD, Perez-Oliva AB, Rodriguez-Ruiz L, et al. Inflammasome regulates hematopoiesis through cleavage of the master erythroid transcription factor GATA1. *Immunity.* 2019;51(1):50-63.e5.
38. Ribeil JA, Zermati Y, Vandekerckhove J, et al. Hsp70 regulates erythropoiesis by preventing caspase-3-mediated cleavage of GATA-1. *Nature.* 2007;445(7123):102-105.
39. Li W, Yuan J. Targeting RIPK1 kinase for modulating inflammation in human diseases. *Front Immunol.* 2023;14:1159743.
40. Xu YR, Lei CQ. TAK1-TABs complex: a central signalosome in inflammatory responses. *Front Immunol.* 2020;11:608976.
41. Mihaly SR, Ninomiya-Tsuji J, Morioka S. TAK1 control of cell death. *Cell Death Differ.* 2014;21(11):1667-1676.
42. Annibaldi A, Wicky John S, Vanden Berghe T, et al. Ubiquitin-mediated regulation of RIPK1 kinase activity independent of IKK and MK2. *Mol Cell.* 2018;69(4):566-580.e5.
43. Malireddi RKS, Gurung P, Mavuluri J, et al. TAK1 restricts spontaneous NLRP3 activation and cell death to control myeloid proliferation. *J Exp Med.* 2018;215(4):1023-1034.
44. Malireddi RKS, Gurung P, Kesavardhana S, et al. Innate immune priming in the absence of TAK1 drives RIPK1 kinase activity-independent pyroptosis, apoptosis, necroptosis, and inflammatory disease. *J Exp Med.* 2020;217(3):jem.20191644.
45. Wang Y, Karki R, Mall R, et al. Molecular mechanism of RIPK1 and caspase-8 in homeostatic type I interferon production and regulation. *Cell Rep.* 2022;41:111434.
46. Runde AP, Mack R, Breslin JP, et al. The role of TBK1 in cancer pathogenesis and anticancer immunity. *J Exp Clin Cancer Res.* 2022;41(1):135.
47. Li W, Shan B, Zou C, et al. Nuclear RIPK1 promotes chromatin remodeling to mediate inflammatory response. *Cell Res.* 2022;32(7):621-637.e7.
48. Zou J, Shi Q, Chen H, et al. Programmed necroptosis is upregulated in low-grade myelodysplastic syndromes and may play a role in the pathogenesis. *Exp Hematol.* 2021;103:60-72.e5.
49. Yamashita M, Passegue E. TNF-alpha coordinates hematopoietic stem cell survival and myeloid regeneration. *Cell Stem Cell.* 2019;25(3):357-372.e7.
50. Pietras EM, Mirantes-Barbeito C, Fong S, et al. Chronic interleukin-1 exposure drives haematopoietic stem cells towards precocious myeloid differentiation at the expense of self-renewal. *Nat Cell Biol.* 2016;18(6):607-618.